

Arctic melt ponds and bifurcations in the climate system

Ivan Sudakov ^{*1}, Sergey A. Vakulenko^{2,3}, and Kenneth M. Golden¹

¹Department of Mathematics, University of Utah

²Institute of Problems in Mechanical Engineering, Russian Academy of Sciences

³University ITMO

Abstract

Understanding how sea ice melts is critical to climate projections. In the Arctic, melt ponds that develop on the surface of sea ice floes during the late spring and summer largely determine their albedo – a key parameter in climate modeling. Here we explore the possibility of a simple sea ice climate model passing through a bifurcation point – an irreversible critical threshold as the system warms, by incorporating geometric information about melt pond evolution. This study is based on a nonlinear phase transition model for melt ponds, and bifurcation analysis of a simple climate model with ice - albedo feedback as the key mechanism driving the system to a potential bifurcation point.

Keywords: sea ice, bifurcations, melt ponds, fractals, pattern formation, phase transitions, climate model.

1 Introduction

Sea ice is not only a sensitive, leading indicator of climate change, it is a key player in Earth's climate system. It also serves as a primary habitat for algal and bacterial communities which sustain life in the polar oceans. Perhaps the most visible, large scale change on Earth's surface in recent decades has been the precipitous decline of the summer Arctic sea ice pack. With this significant loss of a white reflecting surface covering the Arctic Ocean, its albedo or reflectance decreases, and solar radiation is absorbed by the ocean rather than being reflected. This heats the upper ocean, melting even more ice, and so on, which is known as "ice-albedo feedback".

While global climate models predict a general decline in Arctic sea ice over the 21st century, the observed losses have significantly outpaced projections [20, 27]. Improving our predictive capability for the fate of Earth's sea ice cover and its ecosystems depends on a better understanding of important processes and feedback mechanisms. For example, during the melt season the Arctic sea ice cover becomes a complex, evolving mosaic of ice, melt ponds, and open water. The albedo of sea ice floes is determined by melt pond configurations [21, 23, 25]. As ponds develop, *ice-albedo feedback* enhances the melting process. Understanding such mechanisms and their impact on sea ice evolution and its role

*sudakov@math.utah.edu

in the climate system is critical to advancing how sea ice is treated in climate models and improving projections.

Conceptual, or *low order* climate models often introduce feedback through empirical parameterization, for example, taking into account a simple relation between temperature and area of ice covered surface. There is a wide range of such works, including [6, 9, 13, 19]. Usually, ice–albedo feedback was simply associated with a decrease in ice covered area and a corresponding increase in the surface temperature, further decreasing the ice covered area. Given the key role that melt pond formation and evolution plays in sea ice albedo, we note here an apparent lack of incorporation of such features into conceptual models of ice–albedo feedback. Here we note that it is important to explore how melt pond geometry and thermodynamics affect conceptual climate models, and ice–albedo feedback in particular.

While melt ponds form a key component of the Arctic marine environment, comprehensive observations or theories of their formation, coverage, and evolution remain relatively sparse. Available observations of melt ponds show that their areal coverage is highly variable, particularly for first year ice early in the melt season, with rates of change as high as 35 percent per day [23]. Such variability, as well as the influence of many competing factors controlling melt pond and ice floe evolution, make realistic treatments of ice–albedo feedback in climate models quite challenging [23]. Small and medium scale models of melt ponds which include some of these mechanisms have been developed [25, 26], and melt pond parameterizations are being incorporated into global climate models [20].

Moreover, recently it has been found [16] that melt pond geometry has a complex fractal structure, and that the fractal dimension exhibits a transition from 1 to about 2 around a critical length scale of 100 m^2 in area. This behavior should be taken into account in investigating sea ice–albedo feedback.

Given the complex, highly nonlinear character of the underlying differential equations describing climate, it is natural to ask whether the decline of summer Arctic sea ice has passed through a so-called *tipping point*, or irreversible critical threshold as the system progresses toward ice–free summers [1, 9]. A key mechanism potentially driving the system to “tip” is ice–albedo feedback. The main aim of this work is to investigate such a tipping point for a simplified model of sea ice and the climate system which takes into some account the evolution of melt pond geometry and its effect on sea ice albedo.

From the first appearance of visible pools of water, often in early June, the area fraction of sea ice covered by melt ponds can increase rapidly to over 70 percent in just a few days [23], as demonstrated in Fig. 1(a). Moreover, the accumulation of water at the surface dramatically lowers the albedo where the ponds form. A corresponding critical drop-off in average albedo is displayed in Fig. 1(b). The resulting increase in solar absorption in the ice and upper ocean accelerates melting [22], possibly triggering ice–albedo feedback. Similarly, an increase in open water fraction lowers albedo, thus increasing solar absorption and subsequent melting. The spatial coverage and distribution of melt ponds on the surface of ice floes and the open water between the floes thus exerts primary control of ice pack albedo and partitioning of solar energy in the ice–ocean system [8, 23].

The surface of an ice floe is viewed here as a two phase composite of dark melt ponds and white snow or ice. The onset of ponding and the rapid increase in coverage beyond the initial threshold is similar to critical phenomena in the theory of phase transitions. Here we ask if the evolution of melt pond geometry – and sea ice albedo – exhibit universal

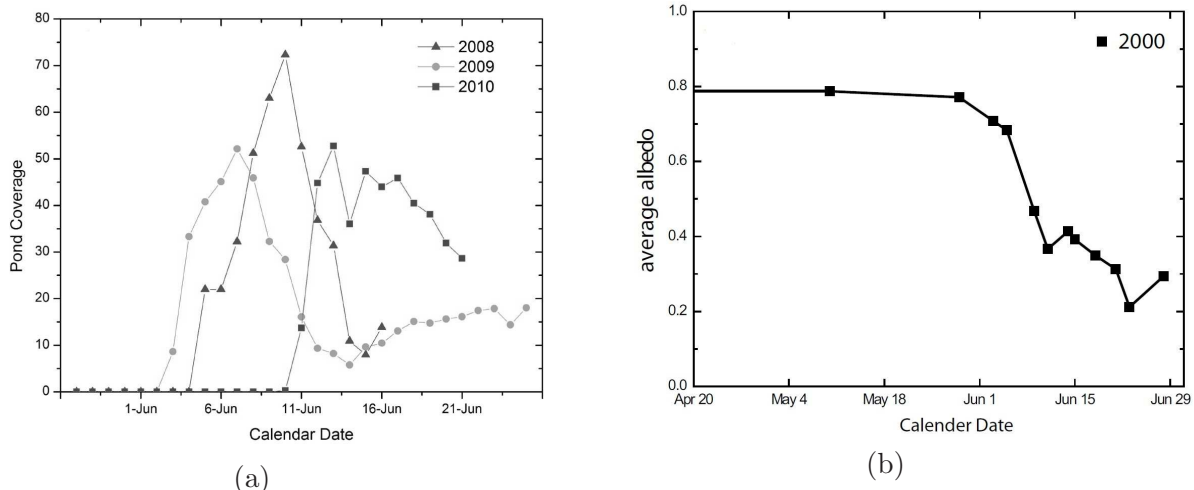


Figure 1: Arctic melt pond coverage vs. calendar date near Barrow, AK in (a), for the years 2008–2010. Average albedo vs. calendar date in 2000 near Barrow is shown in (b) [23]. Each data set exhibits critical behavior at the onset of melt pond formation, similar to the behavior of order parameters characterizing phase transitions in thermodynamics.

characteristics which do not necessarily depend on the details of the driving mechanisms in numerical melt pond models. Fundamentally, the melting of Arctic sea ice is a phase transition phenomenon, where a solid turns to liquid, albeit on large regional scales and over a period of time which depends on environmental forcing and other factors. We thus look for features which are mathematically analogous to related phenomena in the theories of phase transitions and composite materials.

A natural approach to explore the evolution of melt pond geometry is the use of phase field equations, such as the Ginzburg–Landau model [4]. It was originally developed in the context of superconductivity, yet has been used in the study of many phase transition and pattern formation problems. The two main functions of interest are the order parameter $\psi = \psi(x, y, z, t)$ and the temperature $T = T(x, y, z, t)$, for $(x, y, z) \in \mathfrak{R}$ for some region $\mathfrak{R} \subset \mathbb{R}^3$, and $t \geq 0$. In the case of melt ponds, we have two states of different phases, ice and water. The frozen state is characterized by $\psi = -1$ and the melted state by $\psi = +1$. We investigate the melt pond problem by studying the evolution of the interface separating the melted and frozen states. Let us note that using asymptotic methods, the classical Stefan and Hele-Shaw systems can be obtained from the Ginzburg-Landau model in the limit of a sharp interface [4]. We believe that this sharp interface limit should be quite relevant for the melt pond problem.

Further, basing our approach on this nonlinear phase transition model in the 2D case, we obtain an expression for the rate of change of the melt pond radius. It can be extended to the 3D case taking into account the vertical transfer of water to the ocean through ice under a hydraulic head. After that, we introduce the expression for albedo of the ice-covered surface and investigate through the melt pond radius how the unexpected fractal geometry of melt ponds [16] can influence the formula for albedo of the ice covered surface.

As the next step, we consider a standard conceptual climate model – an ordinary differ-

ential equation (ODE) [13] with ice–albedo feedback taking into account the albedo of melt ponds. We modify this model assuming a stochastic distribution of melt pond radii, based on the Fokker-Plank equation. After that we investigate equilibria of the resultant stochastic ODE under the key assumption that the surface temperature is a slow function of time relative to melt pond radius. Different bifurcation regimes were obtained for this model. One of them may be quite interesting for climate applications, where the temperature of this system is stabilized only due to the fractal transition in melt pond geometry.

2 Evolution of melt ponds

2.1 Two-dimensional case

The complexity of the hydrology and thermodynamics of melt pond formation is the basis for the use of sophisticated numerical models of melt pond evolution [25, 26]. We do not discuss here the details of the thermodynamic processes in sea ice leading to the formation of the melt ponds. However, our initial considerations of melt ponds will be based on the following geometrical property of melt ponds. Typically, developed ponds have [11, 23] horizontal sizes (R) on the order 50-1000 m, and a small depth (z) of 0.1–0.8 m, i.e. a melting layer has a small but non-zero thickness. Following [4] we can use phase transition models when the melting layer has a small but non-zero thickness and a large horizontal dimension.

We introduce a cylindrical domain $D = \Omega \times [0, h]$, where Ω is a sub-domain of the $2D$ sphere corresponding to the sea ice surface, (x, y) are coordinates on Ω , and $z \in [0, h]$. The surface temperature of melting ice $T = T(x, y, z, t)$ is the unknown function. We assume that $h \ll L$, where $L = \text{diam}(\Omega)$ and that the boundary of Ω is a smooth curve. We denote by $l(x, y, t)$ the melting front position, the front surface is defined by $z = l$. To study melting problems, usually one uses the classical Stefan problem [4]. However, this approach is difficult to apply without substantial numerical work. Moreover, in this approach the interface width is zero. Since our goal is to obtain some analytical relations, following [4], we use an improved nonlinear approach, where the interface width is small (but is not zero!).

We introduce an order parameter which equals 1 in the ice, -1 in the water and is close to 0 at the ice-water interface. We denote this order parameter by $\psi = \psi(x, y, z, t)$. We use the following equations for the two unknown functions ψ, T :

$$T_t = K \Delta T - \frac{b}{2} \psi_t, \quad (1)$$

$$\alpha \xi^2 \psi_t = \xi^2 \Delta \psi + a^{-1} g(\psi) + 2(T - \theta), \quad (2)$$

where g is typical double well potential, θ is the temperature of the phase transition, K is the average thermal diffusivity of this media, b is a dimensionless latent heat; α (related to a microscopic relaxation time), $a > 0$ (the well depth), and ξ (represents the molecular forces) are dimensionless parameters coming from microscopic theory of phase transition [4]. This model allows us to describe the melting zone of non-zero width. To explain the main idea of the front formation in this model, let us consider the $1D$ variant of (2), removing the

term with the temperature:

$$\alpha\xi^2\psi_t = \xi^2\psi_{nn} + a^{-1}g(\psi), \quad (3)$$

where we assume that the front moves along some notional n line. This equation has the kink solution $U(n) = \tanh(n - vt/l^*)$, where $l^* = a^{-1/2}\xi^{-1}$ is a parameter that defines the front width, v is the velocity [12]. The function $U(n)$ is smooth and well localized at $z = 0$. If $g = 0.5(\psi - \psi^3)$, $v = 0$ and $U(n) = \tanh(n/l^*)$. To describe the influence of $2(T - \theta)$, we can apply the perturbation theory. The front appears at a point, where $T \approx \theta$, i.e., at the melting temperature.

We have the following boundary conditions at the bottom of the pond $z = h$,

$$\tilde{T}_z(x, y, h, t) + \tilde{b}(x, y)\tilde{T}(x, y, h, t) = T_d(x, y, t), \quad (4)$$

$$\psi(x, y, h, t) = -1, \quad (5)$$

and on the surface $z = 0$,

$$T(x, y, 0, t) = T_0(x, y, t), \quad \psi(x, y, 0, t) = 1. \quad (6)$$

Here, \tilde{T} is the temperature on the depth, \tilde{b} is a thermal coefficient, T_d and T_0 are the boundary functions of temperature.

The three dimensional problem (1), (2), (4), (5) and (6) for kink propagation is extremely difficult. However, we can use asymptotic approaches according our assumption about melt pond geometry. Then we can suppose that the ice-water interfaces are quasi one-dimensional, and they can be described by kink solutions $U(n)$, where n is the normal distance between the interface surface (where $\psi = 0$) and the point (x, y, z) . Following [5, 18, 29] we obtain the relation

$$v^*(x, y, z, t) = \delta - \mu\chi(x, y, z, t), \quad (7)$$

where v^* is the normal melting front velocity at the point (x, y, z) , χ is the mean front curvature at this point, μ is a positive coefficient, and δ is non-perturbed kink velocity. The quantity δ can be expressed via microscopic parameters a and ξ however, it is simpler to find this quantity by experimental data since δ determines the main contribution in the pond area increasing. To express δ via microscopic parameters, for small curvatures we can use a one-dimensional approximation of these equations where T, ψ depend on n and t where $n(x, y, z, t)$ is the distance between the observation point $M = (x, y, z)$ and the front. We suppose here that n has a sign, i.e, $n > 0$ if M is beyond the front and $n < 0$ if M is behind the front. Then, up to small corrections proportional to $O(\chi)$, one has $\nabla = \partial/\partial n$, and $\nabla^2 = \partial^2/\partial n^2$. Assume, moreover [29], that the melting front can be described by a slowly moving traveling wave, $\psi = \Psi(z)$, where $z = n - vt$ is a new variable and where the velocity $v = \delta$ is small. Then (1), (2) can be transformed into

$$KT_{zz} = \frac{bv}{2}\Psi_z, \quad (8)$$

$$-v\alpha\xi^2\Psi_z = \xi^2\Psi_{zz} + a^{-1}g(\Psi) + 2(T - \theta). \quad (9)$$

Following some standard calculations [29], one obtains $v = \text{const} \int_{-\infty}^{\infty} (T(z) - \theta)\Psi_z dz$ which allows us to find $v = \delta$ as a function of the microscopic parameters α, a, ξ, b .

For $\delta = 0$, (7) describes so-called *mean curvature flows*, which have been well studied in the literature [3, 7, 10, 14, 18]. Such a flow also occurs if we eliminate temperature from our equations. Actually, relation (7) also is a nontrivial nonlinear equation, even in the 2D-case. Nonetheless, it is much simpler than the original problem (1), (2), (4), (5) and (6) and we will see that relation (7) entails remarkable consequences that can be checked experimentally.

We are planning to consider the planar case. In this case, our fronts are curves. All fronts are closed curves, which initially are not too different from circles, and approach circles for large times. For circular fronts of radius $R(t)$, equation (7) takes the form

$$\frac{dR}{dt} = \delta - \mu R^{-1}, \quad (10)$$

which can be solved explicitly. This equation can be resolved analytically and the solution describes growing ponds of a circular form.

2.2 Three dimensional effects and melting area

Some actual melt ponds can be thought of as three dimensional lenses. In [23] some important effects are described and experimental data are presented. It is shown that there is a vertical transfer of water in the ocean through ice under a hydraulic head, which is proportional to the depth of the lens. We can assume that on average this depth is proportional to the pond radius R . Therefore, due to this effect, a rough estimate of the rate dW/dt of the water mass in the pond is $-\beta W$. Since $W = \text{const}R^3$, we have the following contribution R_w of this effect into dR/dt : $R_w = -\gamma R$. Taking into account this effect, we change (10) into the form

$$\frac{dR}{dt} = \delta(T) - \gamma(T)R - \mu R^{-1} = P(R, T), \quad (11)$$

where we suppose that δ and γ depend on the temperature and $\mu > 0$ is a small parameter.

Note that (11) involves a singularity at $R = 0$. Indeed, this equation is not accurate for small enough R since it is derived under the condition that the curvature radius is much larger than the interface width. Formally, if the initial $R(0)$ is small enough, we have that the solution $R(t)$ of (11) converges to zero as $t \rightarrow \infty$. Physically, this means that the ponds of small sizes are refreezing. For example, abrupt change of current weather in the summer time can lead to refreezing of small melt ponds. In addition, circular melt ponds on multiyear ice have a tendency to refreezing by the end of the season [24]. It is clear that actually small ponds have this refreezing property, independent of correctness (11). We can then make precise the form of P for some critical radius of refreezing R_0 in (11) as follows:

$$P(R, T) = -\gamma_0 R, \quad R < R_0, \quad (12)$$

(γ_0 is a parameter corresponding to the refreezing case) and for $R > R_0$ we have (11).

3 Melt ponds and albedo

Albedo is the reflecting power of a surface. Material properties, surface topography, and other properties of the surface influence albedo as well as related feedback mechanisms. We

will involve melt ponds in the feedback by means of area. For this aim we apply (7) to study the melt ponds area. Relation (10) entails consequences that can be checked experimentally.

Experimentally [11], the albedo of the surface is

$$A = A_0(1 - S_r) + B_0 S_r = A_0 - (A_0 - B_0)S_r, \quad (13)$$

where A_0 is an average albedo of ice area, B_0 is an average albedo of melt ponds, the percentage of the surface covered by ponds: $S_r = \frac{\bar{S}}{S_i}$ with \bar{S} - the average area of all melt ponds, S_i - the average ice area. Thus, we have obtained the formula for albedo involving area of the surface covered by melt ponds. It takes into account melt pond radius dynamics.

As was shown in [16] that the melt pond perimeter Π can be defined approximately by

$$\Pi \sim \sqrt{S}^D, \quad (14)$$

here S - area of ponds, D - the fractal dimension. The authors have observed a transition from $D = 1$ to $D \approx 2$ as the ponds grow in size, with the transitional regime centered around 100 m^2 . According to [16] there exist three regimes:

- A) $S < 10 \text{ m}^2$; then we observe simple ponds with smooth boundaries and $D \approx 1$;
- B) $10 \text{ m}^2 < S < 1000 \text{ m}^2$; corresponding to transitional ponds where complexity increases rapidly with size;
- C) $S > R_F = 1000 \text{ m}^2$; complex, self-similar case, where pond boundaries behave like space filling curves with $D \approx 2$.

Using these facts we compute the melt pond area as follows. For the averaged radius $R(t) < R_F$ we assume that melts ponds are close to circles or ellipses. Then we we define the area of melt ponds by

$$S(\mathbf{R}) \approx \pi c_1 \sum_{i=1}^N R_i(t)^2, \quad S < S_* = N\pi c_1 R_F^2 \quad (15)$$

supposing that the ponds are close to circular form, the coefficient c_1 takes into account a deviation of circular form. Here $\mathbf{R} = (R_1(t), \dots, \dots R_N(t))$ is a vector of pond radii and N is the number of the ponds. For $R > R_F$ the ponds become long and narrow. Then we use the relation

$$S(\mathbf{R}) \approx c_2 \sum_{i=1}^N R_i(t), \quad S > S_*, \quad (16)$$

where c_2 is a constant. Here we suppose that the ponds are close to long and narrow ellipses and R is the length of the long semi-major axis. These ellipses remind one of rivers rather than the usual circular ponds. Then one can expect that the area of such a river of length R is proportional to R .

4 Simple climate model with ice–albedo feedback for melt ponds

In previous sections, we have obtained expressions for the albedo involving the percentage of the surface covered by melt ponds, which depends on the area of the ponds. In turn,

the area evolution depends on melt pond radius dynamics. This can be exploited in a conceptual climate model. Such models are based on an ice–albedo feedback that allows albedo to be temperature dependent. These models couple the albedo to the global energy balance through inclusion of heat transport [6, 19]. In this section we show how these models can be parameterized taking into account melt pond radius dynamics. It is based on a relationship between albedo, melt pond radius, and temperature. It allows us to find a climate bifurcation point related to melt ponds, and estimate climate sensitivity provided that melt ponds play a key role in the mechanism of ice–climate feedback.

A simple climate model is a one-dimensional system which can be described [13] by

$$\frac{dT}{dt} = \frac{1}{\lambda}(-\epsilon\sigma T^4 + \frac{\mu_0}{4}I_0(1 - A)), \quad (17)$$

where λ is thermal inertia, T is surface temperature, t is time, and A is the albedo of the surface. The left term characterizes the time-dependent behavior of the climate system, usually taken to mean an average surface temperature. Surface temperature changes as a result of an imbalance in radiative heat transfer. In the right part, the first term is outgoing emission as well as the second term represents incoming solar radiation. Generally, incoming solar radiation to earth’s surface should depend on total solar radiation incident on earth (μ_0), and the solar constant (I^0) as well as surface albedo. On the other side, outgoing emission can be described through the fourth power of temperature, the effective emissivity (ϵ) and a Stefan-Boltzmann constant (σ).

Substituting the formula for A via the radius, we have finally the following system for R_i, T :

$$\frac{dT}{dt} = f(R_i, T), \quad (18)$$

where

$$f(R_i, T) = \frac{1}{\lambda}(-\epsilon\sigma T^4 + \frac{\mu_0}{4}I_0(1 - A_0 + \bar{c}(A_0 - B_0)S(T)/S_i),$$

and

$$dR_i = P(R_i, T)dt + 2\kappa d\omega_i, \quad (19)$$

where $\bar{c} = A_0 - B_0 > 0$, $i = 1, \dots, N$ and κ is a parameter. Here, observing that pond growth can be viewed as a stochastic process, we use the Langevin equation for R_i , where $d\omega_i$ are independent standard Wiener processes. Since $N \gg 1$ we can also use the Fokker-Planck equation for the pond radius distribution $\rho(R_i, t)$:

$$\frac{\partial \rho}{\partial t} = -\frac{\partial P(R_i, T)\rho}{\partial R_i} + \kappa^2 \frac{\partial^2 \rho}{\partial R_i^2}. \quad (20)$$

This nonlinear climate model can be reformulated as a stochastic dynamical system. Note that for $R_i > R_0$, $\kappa = 0$ (when stochastic effects are absent), and with increasing $\delta(T)$ one has

$$\frac{\partial f(R_i, T)}{\partial R_i} > 0, \quad \frac{\partial P(R_i, T)}{\partial T} > 0.$$

This means that the system (18) is cooperative. Therefore, due to fundamental results of M. Hirsch [15], this system cannot exhibit oscillating, nontrivial (with non-zero melt pond area)

solutions and the Andronov–Hopf bifurcations [2]. All trajectories converge to equilibria and the attractor is a union of these equilibria.

This observation allows us to compute the pond area S for large times. In physically realistic situations $N \gg 1$, and we can simplify the approximations (15) and (16). We can transform these relations as follows

$$S \approx S_c = \pi c_1 N \int_0^\infty R_i^2 \rho(R_i, t) dR_i, \quad (21)$$

for $S_c < s_* N$, where $s_* = \pi c_1 R_F^2$, and c_1 is a constant taking into account the deviation from the circular pond form.

After the fractal transition one has

$$S \approx S_F = c_2 N \int_0^\infty R_i \rho(R_i, t) dR_i, \quad (22)$$

for $S_c < s_* N$. Here $\rho(R_i, t)$ can be defined by equation (20).

5 Analysis of the system for temperature and ponds

Equilibria of the system (18) and (19) for $\kappa = 0$ can be found as follows. For fixed temperature T we compute quasiequilibria $R_i(T)$ setting $P(R_i, T) = 0$. Equation $P(R_i, T)$ has three roots:

$$R_0 = 0, \quad R_+(T) = \frac{\delta(T) + \sqrt{\delta(T)^2 - 4\gamma\mu}}{2\gamma} \quad (23)$$

$$R_-(T) = \frac{\delta(T) - \sqrt{\delta(T)^2 - 4\gamma\mu}}{2\gamma} \quad (24)$$

For small μ we can use asymptotics

$$R_+(T) \approx \frac{\delta(T)}{\gamma(T)}, \quad R_-(T) = \frac{\mu}{\delta}. \quad (25)$$

Note that the roots R_0 and R_+ correspond to stable resting points (local attractors) of a semiflow defined by equation (18) while R_- is a saddle point. Therefore, the dynamics of (18) can be described as follows: if the initial state $\dot{a} = R_i(0)$ satisfies $R_i(0) < R_-$, then $R_i(t) \rightarrow 0$ for large times t , otherwise, $R_i \rightarrow R_+$.

Our key assumption is that T is a slow function of time relative to $R_i(t)$, i.e., the melting process for ponds is fast while changing of the related climate system is slow.

Note that if this assumption does not hold we can observe an interesting effect. Namely, potentially we can have an exponentially large number N of equilibria, since, depending on initial data, $R_i = 0$ or $R_+(T)$.

Under such an assumption computing equilibria for the temperature T becomes a feasible problem even in the stochastic case $\kappa > 0$. In fact, then (using classical results of dynamical systems theory) we solve the Fokker-Planck equation (20) for each fixed T , after which we substitute the results in (17) and find the equilibria for T . So, let us fix T in equation (20).

It is well known that $\rho(R_i, t) \rightarrow \rho_{eq}$ for large times t , where ρ_{eq} is an equilibrium distribution defined by

$$\rho_{eq} = C(T) \exp(-\kappa^{-2}V(R)), \quad (26)$$

with

$$V(R) = \delta(T)R - 0.5\gamma(T)R^2 - \mu \log(R),$$

where $C(T)$ is a factor such that $\int_0^\infty \rho_{eq}(R)dR = 1$. We have then

$$S_c = \pi c_1 N C(T) \int_0^\infty R^2 \exp(-\kappa^{-2}V(R))dR, \quad (27)$$

for $S_c < s_*N$, and

$$S_F = c_2 N C(T) \int_0^\infty R \exp(-\kappa^{-2}V(R))dR, \quad (28)$$

for $S_c > s_*N$. Therefore, for small κ we obtain the following relations for the pond area S (using that the function ρ_{eq} is well localized at $R = R_+(T)$)

$$S(T) = S_c = C_0 N (R_+(T)/R_F)^2, \quad (29)$$

for $S_c < s_*N$, and

$$S(T) = S_F = C_0 N R_+(T)/R_F \quad (30)$$

for $S > C_0N$. Here C_0 is a constant and R_F is the radius of the fractal transition. We assume that $R_+(T)$ is an increasing function of T

$$\frac{dR_+(T)}{dT} > 0. \quad (31)$$

This assumption looks natural. Note that $S(T)$ has such properties. This function is continuous and has a derivative $dS/dT = S'(T)$, which has a break at the temperature T_* such that $S(T_*) = R_F$. Indeed, we have the derivatives with two-sided limits of the temperature ($(T_* - 0)$ and $(T_* + 0)$)

$$\frac{dS(T_* - 0)}{dT} = 2C_0N \frac{dR(T_*)}{R_F dT}, \quad \frac{dS(T_* + 0)}{dT} = C_0N \frac{dR(T_*)}{R_F dT}. \quad (32)$$

For the temperature T we obtain then the evolution equation

$$\frac{dT}{dt} = G(T), \quad (33)$$

where

$$G(T) = \frac{\epsilon\sigma}{\lambda}(-T^4 + Q(T)), \quad Q(T) = \frac{\bar{c}\mu_0 I_0}{4\epsilon\sigma}((\bar{c})^{-1}(1 - A_0) + \zeta(T)), \quad (34)$$

and $\zeta(T) = (A_0 - B_0)\frac{S(T)}{S_i}$.

The equilibria of this equation are defined by

$$G(T) = 0. \quad (35)$$

These equilibria are intersections T_j of the curves $-\epsilon\sigma T^4$ with $Q(T)$. If for T_j one has

$$4\epsilon\sigma T_j^3 > Q'(T_j),$$

then the intersection is a stable equilibrium and thus a local attractor, otherwise this equilibrium is a saddle point.

Note that the function $Q(T)$ grows faster in T for smaller T while the averaged pond radius less than the critical value around R_F . This means that early in the warming cycle we observe fast growth and afterwards when the ponds become fractals, the growth in $Q(T)$ is slower. This result is consistent with experimental data [23].

Depending on the parameters such as $\beta = \frac{\bar{c}\mu_0 I_0}{4\epsilon\sigma}$, $\bar{A} = (\bar{c})^{-1}(1 - A_0)$ and others there are two cases: **(I)** absence of equilibria, when the temperature keeps increasing without bound; and **(II)** a single equilibrium which serves as a global attractor.

Suppose that $Q(T) \approx a_0 + \text{const}T^r$, where r is any real number, a_0 is a parameter. One can show (we omit a formal proof) that then the case of two equilibria is impossible. Let $r > 4$. Then for large T the function $Q(T)$ always increases faster than T^4 . Therefore, if β is sufficiently large we have situation **I**.

The second case is $r < 2$. Then for large T the function $Q(T)$ always increases more slowly than T^4 . Thus in this case we always have a single stable equilibrium (situation **II**).

The most interesting case is $r \in (2, 4)$. Then first $Q(T)$ increases faster than T^4 , thus it is possible that we have no intersections of the graphs of T^4 and $Q(T)$. However, due to the discontinuity of $S'(T)$ (see above), i.e., due to the fractal transition, we can obtain a single equilibrium (see Fig. 2a) for some β . In this case the temperature is stabilized only due to the fractal transition. So, we observe here a stable regime and unstable one.

A more complicated bifurcation picture occurs if we assume that $Q(T)$ is almost constant for $T < T_b$, and increasing for $T > T_b$. This condition looks natural since for low temperatures melt ponds are frozen.

We can take the following approximation: $Q(T) = a^* + b^*R_+^2(T)$, where $R_+(T) = c_0$ for $T < T_b$ and $R_+(T) = (c_0 + c_*(T - T_b)(1 + (T - T_b))^{-1})$ for $T < T_F$, where T_F is the temperature corresponding to the fractal transition and T_b is the initial melting temperature of melt ponds. For $T > T_F$ we have $Q(T) = a^* + b^*R_F R_+(T)$, where $R_F = R_+(T_F)$ is the averaged radius corresponding to the fractal transition. Such an approximation means that we use linear approximations for $\delta(T)$ and $\gamma(T)$ for $T > T_b$. In this case, a pitchfork bifurcation is possible (see Fig. 2b). Note that the transition from a single solution to three occurs if the parameter I_0 changes (it is equivalent to a change of ϵ). Parameters which were used for numerical simulations are presented in Table 1. A lot of them were found during analysis of the literature presented in References.

6 Discussion and Conclusions

At the beginning of this section, we would like to discuss some features of the melt pond system related to the transition in the fractal dimension. As you can see above this important property of melt ponds can allow us to find new regimes in the dynamics of the simple climate model. Some assumptions related to the critical radius of the fractal transition were used in the calculation of the simple climate model. Here, we can show that the transition

Table 1: Parameters in the simple climate model

Meaning	Name	Value
Initial melting temperature of melt ponds	T_b	275.00 K
Temperature corresponding to the fractal transition	T_F	282.00 K
Thermal inertia	λ	$10^8 \text{ kg} \cdot \text{K}^{-1} \text{ s}^{-2}$
StefanBoltzmann	σ	$5.67 \cdot 10^{-8} \text{ J} \cdot \text{s}^{-1} \text{ m}^{-2} \text{ K}^{-4}$
Incoming solar energy	$I_0/4$	340.00 $\text{W} \cdot \text{m}^{-2}$
Effective emissivity	ϵ	0.62
Average albedo of ice area	A_0	0.68
Average albedo of melt ponds	B_0	0.52
Average albedo after the fractal transition	A_F	0.30
Change in albedo due to the fractal transition	A_m	0.19
Coefficient in approximation of $Q(T)$	a^*	1.00
Coefficient in approximation of $Q(T)$	b^*	10.00
Parameter which is equal to $R_+(T)$ for $T < T_b$	c_0	1.00
Parameter which is related to $R_+(T)$ for $T < T_F$	c_*	5.00

in empirical formula (14) can be obtained from the rigorous pattern formation theory. To this end, we use the Kuramoto-Sivashinsky equation [17] that allows us to demonstrate that beginning with a critical radius, the melting front becomes unstable with respect to perturbations along the front.

To describe the beginning of the fractal boundary growth, we can use the linearized Kuramoto-Sivashinsky equation:

$$\tilde{h}_t = -m_0 \tilde{h}_{zz} - n_0 \tilde{h}_{zzzz}, \quad (36)$$

where \tilde{h} is a normal displacement along the front; z is the coordinate along the front; $z \in [0, P]$; P is a pond perimeter, m_0 and n_0 are positive coefficients. Since the pond boundary is a closed curve, we set P -periodic boundary conditions for \tilde{h} . Then the nontrivial solution of (36) is

$$\tilde{h} = P_0 \exp(ikz + \beta_0(k)t), \quad \beta_0 = m_0 k^2 - n_0 k^4, \quad (37)$$

where $k = 2\pi m_1/P$, m_1 is a positive integer, P_0 is a constant. Hence, the minimum k is $k_{min} = 2\pi/P$. If $\beta_0(k_{min}) < 0$ for all k then the front is stable because all perturbations decrease exponentially. If $\beta_0(k_{min}) > 0$ we have an instability and \tilde{h} increases with an exponential rate. Clearly, it must be a sufficiently large radius. Thus, one can show that the Kuramoto-Sivashinsky equation describes fractal growth [17]. We thus obtain the next equation that defines the critical perimeter found in [16]:

$$P_c = 2\pi(n_0/m_0)^{1/2}. \quad (38)$$

Furthermore, we also would like to discuss the critical transition in melt pond albedo. Here, we are taking into account that the melt pond radius is a fast variable, and the surface temperature (time-averaged) is a slow variable. Therefore, the mean radius depends on the temperature. Also, $\delta(T)$ and $\gamma(T)$ in equation (11) are close to constant (or slightly changing

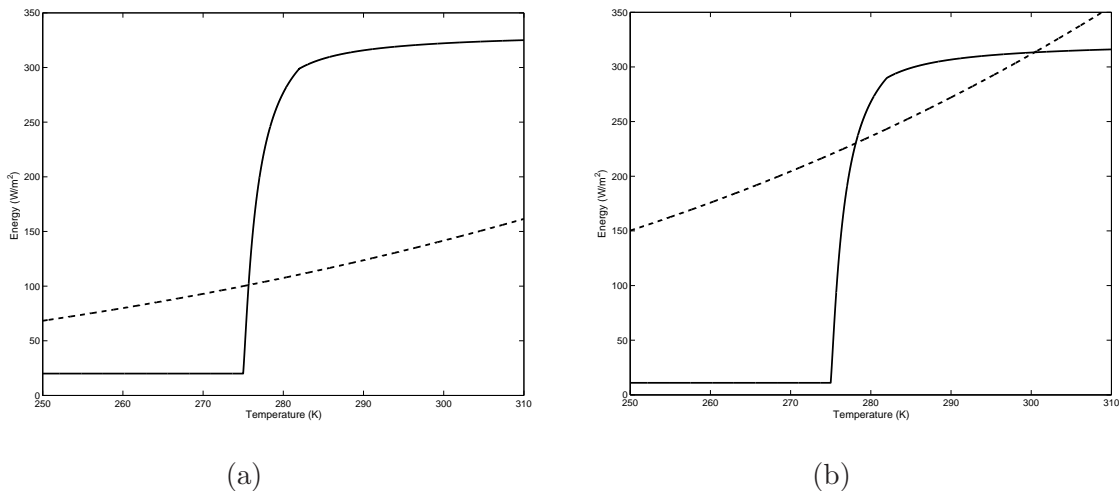


Figure 2: There are the cases of a single equilibrium (a) and three equilibria (b). The dashed curve is related to the term with T^4 of the equation (34) and the solid curve is $Q(T)$. The steady states of T are intersections of these curves.

as a function of T). In this case, the radius is a smooth function of the temperature. When the critical radius is changing due to the fractal transition, functions of melt pond area have a jump at this point:

$$S = \begin{cases} S_c, & R_i < R_F \\ S_F, & R_i > R_F \end{cases} \quad (39)$$

According to formula (13) the albedo depends linearly on area. So, we can approximate albedo as a hyperbolic tangent of the average surface temperature (see Fig. 3):

$$A(\bar{T}) \approx A_F + A_m \tanh(T_\Delta) \quad (40)$$

where A_F is the albedo of the surface after the fractal transition, and A_m - the constant corresponds to the change in albedo due to the fractal transition, T_Δ - changing in the surface temperature due to the fractal transition [23]. Previously, this formula was introduced empirically, based on the observation data. However, we may see physical interpretation of this phenomenon: the transition in fractal dimension of melt ponds affects on shape of albedo curve.

Thus, we have addressed here some fundamental questions related to our understanding of the role of sea ice in the climate system. First of all, we considered how geometrical and thermodynamic properties of melt ponds can influence ice - albedo feedback and how it can influence the bifurcation structure of a simple climate model - stochastic ODE.

We applied a nonlinear phase transition model to the study of melt pond formation, and proposed here an approach which can serve as a basis for future investigations of the thermodynamics of melt ponds and their evolution.

We reviewed a simple energy balance climate model using standard methods of dynamical systems theory. We can see different behavior of the climate system in the case of the ice-albedo feedback with melt pond following a stochastic distribution for the radii.

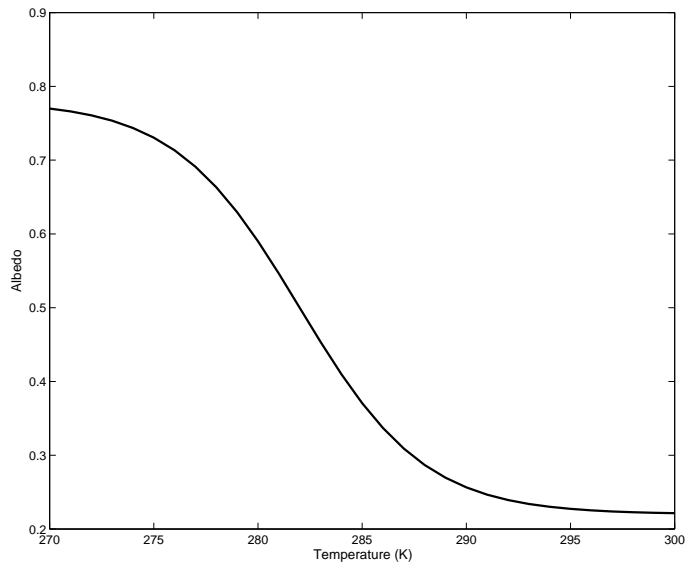


Figure 3: Albedo as a hyperbolic function of the average surface temperature due to the fractal transition in the melt pond geometry.

We concluded that melt ponds in this case can strengthen the positive feedback and lead the climate system through a bifurcation point. As shown by numerical simulations, the melt pond contributions have a significant influence on the temperature state of the climate system.

We would like to emphasize that in this research three scales of the problem were connected. We have tied up micro, macro and global scales through the relation for albedo. Albedo (global scale) contains the area of melt ponds (expressed through radius - macro scale) which in turn is connected to the microscopic parameters of the phase transition in the nonlinear model for melt pond radius evolution. Thus, this research is advancing the scaled approach to tipping points investigations, first presented for permafrost lakes in [28]. Finally, this research should be useful for applied mathematics. It again raises the question of how critical points in phase transition theory can be associated with the tipping points in the theory of dynamical system. Some tools of this model can be useful for the future investigation of this question.

Acknowledgments

We gratefully acknowledge support from the Division of Mathematical Sciences and the Office of Polar Programs at the U.S. National Science Foundation (NSF) through Grants DMS-1009704, ARC-0934721, and DMS-0940249. We are also grateful for support from the Office of Naval Research (ONR) through Grant N00014-13-10291. We would like to thank the NSF Math Climate Research Network (MCRN) as well for their support of this work. Finally, this research was also supported by the Government of the Russian Federation

through mega-grant 074-U01, President's grant MK-128.2014.1, and RFBR's grant 14-01-31053.

References

- [1] Abbot, D., Silber, M., & Pierrehumbert, R. (2011) Bifurcations leading to summer arctic sea ice loss. *J. Geophys. Res.*, textbf 116, D19120, doi:10.1029/2011JD015653.
- [2] Arnold, V. I. (1983) *Geometrical methods in the theory of ordinary differential equations*. Grundlehren Math. Wiss., Springer.
- [3] Bronsard, L. & Kohn, R. V. (1991) Motion by mean curvature as the singular limit of Ginzburg-Landau dynamics. *J. Differential Equations*, **90** (2), 211–237.
- [4] Caginalp, G. (1989) Stefan and Hele-Shaw type problems as asymptotic limits of the phase field equations. *Phys. Rev. A*, **39**, 5887–5896.
- [5] Chen, X.(1992) Generation and propagation of interfaces for reaction-diffusion equations. *J. Differential Equations*, **96** (1), 116–141.
- [6] Curry, J. A., Schramm, J. & Ebert, E. E. (1995) On the sea ice albedo climate feedback mechanism. *J. Climate*, **8**, 240–247.
- [7] Ecker, K. & Huisken, G.(1991) Interior estimates for hyper-surfaces moving by mean curvature. *Invent. Math.*, **105** (3), 547–569.
- [8] Eicken, H., Grenfell, T. C., Perovich, D. K., Richter-Menge, J. A. & Frey, K. (2004) Hydraulic controls of summer Arctic pack ice albedo. *J. Geophys. Res. (Oceans)*, **109**(C18), C08007.
- [9] Eisenman, I. & Wettlaufer, J. S. (2009) Nonlinear threshold behavior during the loss of Arctic sea ice. *PNAS*,**106** (1), 28–32. doi:10.1073/pnas.0806887106.
- [10] Evans, L. C., Soner, H. M. & Souganidis, P. E. (1992) Phase transitions and generalized motion by mean curvature. *Comm. Pure Appl. Math.*, **45** (9), 1097–1123.
- [11] Fetterer, F. & Untersteiner, N. (1998) Observations of melt ponds on Arctic sea ice. *J. Geophys. Res.*, **103**(C11), 24821–24835.
- [12] Fife, P. C. & McLeod, J. B. (1977) The approach of solutions of nonlinear diffusion equations to travelling front solutions. *Arch. Rat. Mech. Anal.*, **65**, 335–361.
- [13] Fraedrich, K. (1979) Catastrophes and Resilience of a zero-dimensional climate system with ice-albedo and greenhouse feedback. *Q. J. R. Meteorol. Soc.*, **105**, 147–167.
- [14] Giga, Y.(2002) *Surface Evolution Equations Level Set Method, Vorlesungsreihe, 44*. Bonn: Rheinische Friedrich-Wilhelms-Universität.
- [15] Hirsch, M. W. (1984) The dynamical systems approach to differential equations. *Bull. A. M. S.*, **11**, 1–64.

- [16] Hohenegger, C., Alali, B., Steffen, K. R., Perovich, D. K. & Golden, K. M. (2012) Transition in the fractal geometry of Arctic melt ponds. *The Cryosphere*, **6**, 1157–1162, doi:10.5194/tc-6-1157-2012.
- [17] Hyman., J. M. & Nicolaenko, B. (1986) The Kuramoto-Sivashinsky equation: A bridge between PDE's and dynamical systems. *Physica D*, **18**, 113–126.
- [18] Mottoni De, P. & Schatzman, M. (1995) Geometrical evolution of developed interfaces. *Trans. Amer. Math. Soc.*, **347** (5), 1533–1589.
- [19] North, G. R. (1975) Theory of energy-balance climate models. *J. Atmos. Sci.*, **32**, 2033–2043.
- [20] Pedersen, C. A., Roeckner, E. Luthje, M. & Winther, J. (2009) A new sea ice albedo scheme including melt ponds for ECHAM5 general circulation model. *J. Geophys. Res.*, **114:D08101**, doi:10.1029/2008JD010440.
- [21] Perovich, D. K., Light, B., Eicken, H., Jones, K. F., Runciman, K., & Nghiem, S. V. (2007) Increasing solar heating of the Arctic Ocean and adjacent seas, 1979-2005: and role in the ice-albedo feedback. *Geophys. Res. Lett.*, **34**, L19505, doi:10.1029/2007GL031480.
- [22] Perovich, D. K., Richter-Menge, J. A., Jones, K. F. & Light, B. (2008) Sunlight, water, and ice: Extreme Arctic sea ice melt during the summer of 2007. *Geophys. Res. Lett.*, **35**, L11501, doi:10.1029/2008GL034007.
- [23] Polashenski, C., Perovich, D., & Courville, Z.(2012) The mechanisms of sea ice melt pond formation and evolution. *J. Geophys. Res. C (Oceans)*, **117:C01001**, doi:10.1029/2011JC007231.
- [24] Sankelo, P., Haapala, J., Heiler, I. & Rinne, E. (2010) Melt pond formation and temporal evolution at the drifting station Tara during summer 2007. *Polar Research*, **29(3)**, 311–321.
- [25] Scott, F. & Feltham, D. L.(2010) A model of the three-dimensional evolution of Arctic melt ponds on first-year and multiyear sea ice. *J. Geophys. Res.*, **115 (C12)**, C12064, doi: 10.1029/2010JC006156.
- [26] Skyllingstad, E. D. & Paulson, C. A. (2007) A numerical simulations of melt ponds. *J. Geophys. Res.*, **112**, C08015, doi:10.1029/2006JC003729.
- [27] Stroeve, J., Holland, M. M., Meier, W., Scambos, T. & Serreze, M. (2007) Arctic sea ice decline: Faster than forecast. *Geophys. Res. Lett.*, **34(9)**, L09591, doi: 10.1029/2007GL029703.
- [28] Sudakov, I. & Vakulenko, S. (2014) A mathematical model for positive permafrost carbon-climate feedback. *IMA J Appl Math*, in press.
- [29] Vakulenko, S. (2013) *Complexity and evolution of dissipative systems; an analytical approach*. Walter de Gruyter.